

Showcasing the search for metalloid tin clusters presented by Prof. Dr Stephan Schulz, Faculty of Chemistry, University of Duisburg-Essen.

Synthesis and solid state structure of a metalloid tin cluster $[\text{Sn}_{10}(\text{trip}_8)]$

Reduction of Sn_2trip_4 with the strong Mg(I) reductant $(\text{LMg})_2$ ($\text{L} = \text{HC}[\text{C}(\text{Me})\text{N}(\text{dipp})]_2$) occurred with tin-carbon bond breaking and formation of a mixed-valent metalloid Sn_{10} cluster containing Sn atoms in the formal oxidation states 0, I and II.

As featured in:



See S. Schulz et al.,
Chem. Commun., 2016, **52**, 12282.



Cite this: *Chem. Commun.*, 2016, 52, 12282

Received 17th August 2016,
Accepted 25th August 2016

DOI: 10.1039/c6cc06770k

www.rsc.org/chemcomm

Synthesis and solid state structure of a metalloid tin cluster $[\text{Sn}_{10}(\text{trip}_8)]^{\dagger}$

J. Wiederkehr, C. Wölper and S. Schulz*

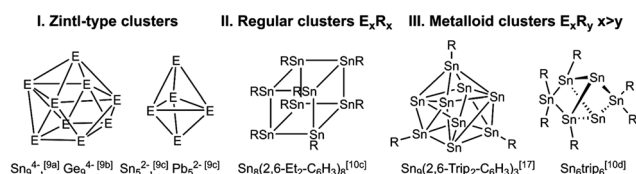
$(\text{trip}_2\text{Sn})_2$ ($\text{trip} = 2,4,6\text{-i-Pr}_3\text{C}_6\text{H}_2$) reacts with $\text{Mg}(\text{I})$ reductants (LMg_2 ($\text{L} = \text{HC}[\text{C}(\text{Me})\text{N}(\text{dipp})]_2$) and ($\text{L}'\text{Mg}_2$ ($\text{L}' = \text{HC}[\text{C}(\text{Me})\text{N}(\text{mes})]_2$) with Sn-C bond cleavage and formation of the novel metalloid tin cluster $\text{Sn}_{10}\text{trip}_8$ **1** or elemental tin. **1**, which contains Sn atoms in the formal oxidation states 0, +I and +II, and the side products LMgtrip (**2**) and $\text{L}'\text{Mgtrip}$ (**3**) were characterized spectroscopically and by single crystal X-ray diffraction.

Metal clusters have been investigated for decades since the understanding of the nature of metal-metal bonds is of fundamental interest in chemistry as well as due to the promising technical applications of nanometer sized metal clusters.¹ Transition metals are particularly suited for the synthesis of clusters due to the presence of $(n+1)s$, $(n+1)p$ and nd orbitals, but main group metal clusters have also received growing interest and their number steadily increased within the last decades.² The development of the co-condensation technique by the Schnöckel group resulted in the synthesis of unforeseen main group metal clusters including so called metalloid clusters, in which the number of metal atoms exceeds the number of ligands.³ These clusters contain “naked” metal atoms which are only bonded to other metal atoms and hence adopt the formal oxidation state 0. Even though the topology of the metal atoms in bulk metals and in metalloid clusters differs, metalloid clusters can be considered as intermediates of the bulk metal formation.⁴

Group 14 (metalloid) clusters have been intensely studied in recent years. They were typically synthesized by reduction reaction of metal complexes RMX_3 (R = organic substituent, X = halide) as was shown for instance for octasilacubanes $[\text{RSi}]_8$,⁵ or starting from metastable metal(I) halide solutions as was demonstrated by Schnepf *et al.* for metalloid germanium and tin clusters including

$\text{Ge}_{18}[\text{Si}(\text{SiMe}_3)_3]_6$, the biggest group 14 metal cluster structurally characterized, to date.^{4,6–8} The vast majority of clusters of the heavier group 14 elements fall into three categories: ligand-free Zintl anions $[\text{E}_x]^{y-}$ ($y = 2, 3$ or 4 , **I**),⁹ from which E_5^{2-} or E_9^{n-} ($n = 2, 3, 4$) are well known, ligand-stabilized neutral clusters E_xR_x (**II**) and metalloid clusters of the general type E_xR_y ($x > y$, **III**).¹⁰ Moreover, Zintl-type anions such as E_9^{4-} ions were *exo*-functionalized with alkyl groups or post-transition metals and the resulting $[\text{RGe}_9]^{3-}$, $[\text{R}_2\text{Ge}_9]^{2-}$, $[\text{RGe}_9\text{Ge}_9\text{R}]^{4-}$, and $[\text{RSn}_9]^{3-}$ clusters represent a link between “metalloid” clusters and traditional Zintl ions.¹¹ Scheme 1 shows selected tin clusters of each category.

Metalloid tin clusters Sn_mR_n ($m > n$) are accessible by controlled disproportionation reaction of monovalent tin halides SnX ($\text{X} = \text{Cl}, \text{Br}$),^{4a} whose synthesis is generally accompanied by the formation of small amounts of SnX_2 , in the presence of sterically demanding organic ligands. However, despite the fascinating results, these reactions are often hard to control. For instance, the reaction of $\text{Sn}(\text{I})\text{Br}$ with LiR' ($\text{R}' = \text{Si}(\text{SiMe}_3)_3$) under slightly different conditions yielded SnR'_3 , $\text{Sn}_3\text{R}'_4$, $[\text{Sn}_4\text{SiR}'_4(\text{SiMe}_3)_2]$, $\text{Sn}_9\text{R}'_2$, $\text{Sn}_{10}\text{R}'_6$ and $\text{Sn}_{10}\text{R}'_4$, respectively.^{8c,12–16} Another synthetic route is the reductive coupling of RSnCl or RSnCl_3 by strong reductants such as alkali metals, KC_8 , or $\text{NaC}_{10}\text{H}_8$, *i.e.* the reaction of $[\text{Sn}[\text{N}(2,6\text{-i-Pr}_2\text{-C}_6\text{H}_3)(\text{SiMe}_3)](\mu\text{-Cl})_2]$ with KC_8 yielded a Sn_{15} cluster.¹⁷ Fischer *et al.* showed that the reaction of SnCl_2 with LGa ($\text{L} = \text{HC}[\text{C}(\text{Me})\text{N}(\text{dipp})]_2$; $\text{dipp} = 2,6\text{-i-Pr}_2\text{-C}_6\text{H}_3$), a redox-active subvalent $\text{Ga}(\text{I})$ species with additional σ -donor properties,¹⁸ yielded metalloid clusters $[(\text{L})\text{ClGa}]_2\text{Sn}_7$ and $[(\text{L})\text{ClGa}]_4\text{Sn}_{17}$, to date the largest metalloid tin cluster.¹⁹



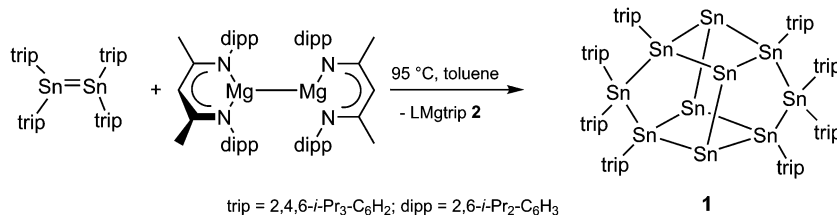
Scheme 1 Different types of group 14 cluster compounds.

Faculty of Chemistry, Inorganic Chemistry, University of Duisburg-Essen,
Universitätsstr. 5-7, S07S03C30, 45114 Essen, Germany.

E-mail: stephan.schulz@uni-due.de; Fax: +49-201-1833830; Tel: +49-201-1834635

† Electronic supplementary information (ESI) available: Experimental procedure and characterization of **1–3**. CCDC 1480548 (**1**), 1499559 (**2**) and 1489510 (**3**). For ESI and crystallographic data in CIF or other electronic format see DOI: 10.1039/c6cc06770k





Scheme 2 Reduction reaction of $\text{trip}_2\text{Sn} = \text{Sntrip}_2$ with $(\text{LMg})_2$ yielding the Sn_{10} cluster **1**.

Unfortunately, the cluster yields are typically low due to the often preferred formation of elemental tin and the reactions can be hardly monitored by *in situ* NMR spectroscopy due to the poor solubility of the starting reagents in organic solvents.

Herein we introduce organodistannenes $\text{R}_2\text{Sn}=\text{SnR}_2$, in which the tin atoms adopt the formal oxidation state +II, as promising starting reagents for the synthesis of metalloid Sn clusters in reactions with strong Mg(I) reductants. $\text{Sn}_{10}\text{trip}_8$ **1** was obtained from the reaction of $(\text{trip}_2\text{Sn})_2$ (trip = 2,4,6-*i*-Pr₃-C₆H₂) with $(\text{LMg})_2$ at 95 °C in toluene as dark red crystals after workup. In contrast, the reaction of the somewhat stronger Mg(I) reducing agent $(\text{L}'\text{Mg})_2$ ($\text{L}' = \text{HC}[\text{C}(\text{Me})\text{N}(\text{mes})]_2$, mes = 2,4,6-Me₃-C₆H₂) only yielded elemental tin. The reactions proceeded with Sn–C bond breakage and subsequent elimination of $\text{HC}[\text{C}(\text{Me})\text{N}(2,6\text{-i-Pr}_2\text{-C}_6\text{H}_3)_2]\text{Mg-2,4,6-i-Pr}_3\text{-C}_6\text{H}_2$ (LMgtrip **2**) or $\text{HC}[\text{C}(\text{Me})\text{N}(2,4,6\text{-Me}_3\text{-C}_6\text{H}_2)_2]\text{Mg-2,4,6-i-Pr}_3\text{-C}_6\text{H}_2$ (L'Mgtrip **3**). **1–3** were characterized by heteronuclear NMR and IR spectroscopy and X-ray crystallography (Scheme 2).

In accordance with the red to purple colour of **1**, the UV/VIS spectrum shows an absorption band at about 540 nm (Fig. S9, ESI†). The ^{119}Sn NMR spectrum (Fig S3, ESI†) of **1** shows three resonances at 134.7, 236.7 and 358.9 ppm, pointing to three magnetically inequivalent Sn atoms. The resonances are shifted to lower field compared to that of $(\text{trip}_2\text{Sn})_2$ (427 ppm). ^{119}Sn NMR resonances are typically not observed for metalloid Sn clusters. Only Power *et al.* reported on ^{119}Sn NMR values in the clusters $\text{Sn}_7(2,6\text{-dipp}_2\text{-C}_6\text{H}_3)_2$ (419.5, 529.7 ppm)^{10e} and $\text{Sn}_8(2,6\text{-mes}_2\text{-C}_6\text{H}_3)_4$ (483.1, 751.7 ppm),^{10a} which are shifted to higher field compared to those observed for **1**. The ^1H NMR spectrum of **1** is rather complex, showing six different resonances for the methine proton of the *i*-Pr groups and several doublets for the Me groups (Fig. S1, ESI†). Temperature-dependent ^1H NMR spectra (Fig. S7 and S8, ESI†) in the range from –80 to +110 °C point to dynamic behaviour of **1** in solution, but an assignment of the resonances is not possible. The reaction of $\text{trip}_2\text{Sn}=\text{Sntrip}_2$ with $(\text{LMg})_2$ was further investigated by *in situ* ^1H NMR spectroscopy. No reaction was observed at ambient temperature even after long reaction times (1d), while the reaction slowly proceeded at 95 °C. Resonances of LMg, **1** and **2** were observed after 6 h (Fig. S5, ESI†), while the reaction was finished after 24 h (Fig. S6, ESI†).

Single crystals of **1–3** were obtained from solutions in *n*-hexane (**1**, Fig. 1) and pentane (**2**, **3**) upon storage at –30 °C for 1 d (**1**, **2**) and 6 d (**3**).²⁰ The Sn_{10} core in **1** contains four “naked” Sn(0) atoms (Sn4, Sn5 and equivalents #1: $-x, -y + 1, -z$), which form a rhombus structure. This core is capped by a chain of three Sn atoms on each side. Alternatively, the structure of **1**

can be described as four edge-sharing five membered rings or as two clamped butterfly-type four-membered rings. Two Sn atoms (Sn2, Sn2#1) carry two ligands (L), hence adopting the formal oxidation state +II, while the remaining four Sn atoms (Sn1, Sn1#1, Sn3, Sn3#1) only carry one ligand and can thus be regarded as Sn(I) atoms.

The structure of the Sn_{10} core of **1** differs from those reported for Sn_{10} clusters, *i.e.* $[\text{Sn}_{10}\text{R}'_4]^{2-}$,⁶ $[\text{Sn}_{10}\text{SiR}'_4(\text{SiMe}_3)_2]^{2-}$,^{14c} $[\text{Sn}_{10}\text{R}'_5]^-$,^{14b} $\text{Sn}_{10}\text{R}'_6$ ($\text{R}' = \text{Si}(\text{SiMe}_3)_3$),^{8c} which adopt distorted centaur polyhedral arrangements with a cubic side and an icosahedral side in accordance with analogous Ge₁₀ and Pb₁₀ clusters such as $(\text{Na}_6[\text{Ge}_{10}\text{Fe}(\text{CO})_4]18\text{THF})^{8b}$ and $(\text{Pb}_{10}[\text{Si}(\text{SiMe}_3)_3]_6)^{21}$. The structure of **1** also differs from that reported for the largest structurally characterized tin cluster, $\text{Sn}_{15}[\text{N}(2,6\text{-i-Pr}_2\text{-C}_6\text{H}_3)(\text{SiMe}_3)_6]$, which contains a body-centred arrangement of the 15 tin atoms.¹⁷ However, edge-sharing five membered rings and butterfly-type four membered rings were previously observed in metalloid germanium clusters such as Ge₁₈R₆⁷ and Ge₁₄R₅^{3–8a,d}.

The Sn–Sn bond lengths within the distorted butterfly-type ring of **1** clearly differ. The Sn3–Sn4 (2.8069(9) Å) and Sn(4)–Sn(1)#1 bonds (2.8243(9) Å) are the shortest Sn–Sn bonds observed in **1**, while the other two (Sn(3)–Sn(5) 2.8854(9), Sn1–Sn5#1 2.8884(9) Å) are the longest ones. The Sn–Sn bonds between the Sn(II) and Sn(I) atoms (Sn(1)–Sn(2) 2.8579(9), Sn(2)–Sn(3) 2.8578(8) Å) fall in between. The *trans*-annular Sn4–Sn5 bond (3.3544(9) Å) within the butterfly-type ring as well as the Sn(4)–Sn(4)#1 bond between these rings (3.2637(12) Å) clearly exceed the sum of the covalent radii (2.80 Å)²² but are shorter than the sum of the van-der Waals radii (4.34 Å).²³ In contrast, the Sn(5)–Sn(5)#1 distance (5.3283(13) Å) is far too long to be considered as attractive interaction. The Sn–Sn bond lengths in Sn_{10} centaur polyhedra typically range from 2.90 to 2.95 Å for the cubic part and 2.95 to 3.05 Å for the icosahedral part,^{6,8c,14b,c} while Sn–Sn bond distances between 2.7992(4) and 3.5729(4) Å were reported for the related Sn_6trip_6 cluster.^{10d} Comparable Sn–Sn bond lengths were observed in other Sn_8 , Sn_9 , Sn_{15} and Sn_{17} clusters.^{10a,15,17,19} The interatomic distances in metallic tin are 3.022 and 3.181 Å.²⁴

Mg(I) compounds are promising reductants for the synthesis of metalloid Sn clusters. They readily react with $\text{trip}_2\text{Sn}=\text{Sntrip}_2$, which contain strong tin-carbon bonds, clearly underlining the strong reducing potential of Mg(I) compounds, which can be further modified by use of different substituents (L, L'). The mes-substituted Mg(I) compound $(\text{L}'\text{Mg})_2$ shows a somewhat higher reducing potential compared to the dipp-substituted derivative $(\text{LMg})_2$. In contrast, the gallanediyl LGa, which reacts with SnCl_2 with formation of tin clusters,¹⁹ failed to react with



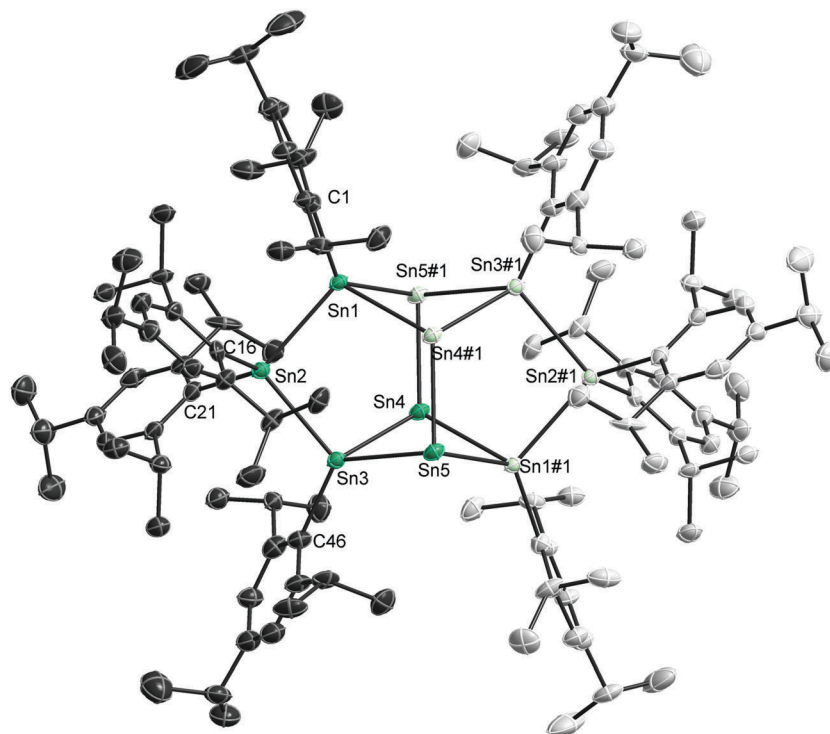


Fig. 1 Solid state structure of **1**; non-H-atoms are shown as thermal ellipsoids at 50% probability levels. H atoms and solvent molecules are omitted for clarity. Light coloured atoms are symmetry equivalent (#1: $-x, -y + 1, -z$). Only the *ipso* C atoms of the trip ligands are labelled. For other atom names please refer to the cif-file. Selected bond lengths [Å] and angles [°]: Sn(1)–Sn(2) 2.8579(9), Sn(2)–Sn(3) 2.8578(8), Sn(3)–Sn(4) 2.8069(9), Sn(3)–Sn(5) 2.8854(9), Sn(4)–Sn(1)#1 2.8243(9), Sn(4)–Sn(5) 3.3544(9), Sn(4)–Sn(4)#1 3.2637(12), Sn(4)–Sn(5)#1 2.8756(8), Sn(5)–Sn(1)#1 2.8883(9), Sn(5)–Sn(5)#1 5.3283(11), Sn(1)–C(1) 2.208(8), Sn(2)–C(31) 2.199(8), Sn(2)–C(16) 2.199(8), Sn(3)–C(46) 2.192(8); Sn(4)#1–Sn(1)–Sn(2) 99.15(2), Sn(4)#1–Sn(1)–Sn(5)#1 71.91(2), Sn(2)–Sn(1)–Sn(5)#1 114.86(3), Sn(3)–Sn(2)–Sn(1) 98.03(2), Sn(4)–Sn(3)–Sn(2) 101.40(2), Sn(4)–Sn(3)–Sn(5) 72.20(2), Sn(2)–Sn(3)–Sn(5) 114.56(3), Sn(3)–Sn(4)–Sn(1)#1 100.43(3), Sn(3)–Sn(4)–Sn(5)#1 120.17(3), Sn(1)#1–Sn(4)–Sn(5)#1 121.80(3), Sn(3)–Sn(4)–Sn(4)#1 81.55(3), Sn(1)#1–Sn(4)–Sn(4)#1 82.75(2), Sn(5)#1–Sn(4)–Sn(4)#1 65.89(2), Sn(4)#1–Sn(5)–Sn(3) 87.39(2), Sn(4)#1–Sn(5)–Sn(1)#1 88.93(2), Sn(3)–Sn(5)–Sn(1)#1 97.09(3).

trip₂Sn=Sntrip₂, clearly proving its weaker reducing properties compared to Mg(I) reagents. Since the distannene and the Mg(I) compounds are both soluble in common organic solvents, a homogeneous reaction route is possible, which provides a better reaction control since the formation of elemental tin can easily be observed. In addition, the reaction can be monitored by *in situ* NMR spectroscopy, which may further help to identify the reaction pathway. We are currently investigating the reduction potential of other soluble reductants toward organotin compounds.

J. Wiederkehr acknowledges financial support (Kekulé-Scholarship) by the Fonds der Chemischen Industrie (FCI) and S. Schulz acknowledges financial support by the University of Duisburg-Essen.

Notes and references

- G. Schmid, M. Baumle, M. Geerkens, I. Heim, C. Osemann and T. Sawitowski, *Chem. Soc. Rev.*, 1999, **28**, 179; Y. Lu and W. Chen, *Chem. Soc. Rev.*, 2012, **41**, 3594.
- S. T. Liddle, *Molecular Metal Metal Bonds*, Wiley VCH, Weinheim, 2015.
- A. Schnepf and H. Schnöckel, *Angew. Chem.*, 2002, **114**, 3682 (*Angew. Chem., Int. Ed.*, 2002, **41**, 3532); H. Schnöckel, *Dalton Trans.*, 2008, 4344; H. Schnöckel, *Chem. Rev.*, 2010, **110**, 4125; H. Schnöckel, A. Schnepf, R. L. Whetten, C. Schenk and P. Henke, *Z. Anorg. Allg. Chem.*, 2011, **637**, 15.
- (a) A. Schnepf, *Chem. Soc. Rev.*, 2007, **36**, 745; (b) A. Schnepf, *New J. Chem.*, 2010, **34**, 2079.
- H. Matsumoto, K. Higuchi, Y. Hoshino, H. Koike, Y. Naoi and Y. Nagai, *Chem. Commun.*, 1988, 1083; H. Matsumoto, K. Higuchi, S. Kyushin and M. Goto, *Angew. Chem.*, 1992, **104**, 1410 (*Angew. Chem., Int. Ed.*, 1992, **31**, 1354).
- C. Schrenk, F. Winter, R. Pöttgen and A. Schnepf, *Chem. – Eur. J.*, 2015, **21**, 2992.
- O. Kysliak, C. Schrenk and A. Schnepf, *Angew. Chem.*, 2016, **128**, 3270 (*Angew. Chem., Int. Ed.*, 2016, **55**, 3216).
- (a) C. Schenk and A. Schnepf, *Chem. Commun.*, 2008, 4643; (b) A. Schnepf and C. Schenk, *Angew. Chem.*, 2006, **118**, 5499 (*Angew. Chem., Int. Ed.*, 2006, **45**, 5373); (c) C. Schrenk, I. Schellenberg, R. Pöttgen and A. Schnepf, *Dalton Trans.*, 2010, **39**, 1872; (d) C. Schenk, A. Kracke, K. Fink, A. Kubas, W. Kloppe, M. Neumaier, H. Schnöckel and A. Schnepf, *J. Am. Chem. Soc.*, 2011, **133**, 2518.
- J. D. Corbett and P. A. Edwards, *J. Am. Chem. Soc.*, 1977, **99**, 3313; L. Xu and S. C. Sevov, *J. Am. Chem. Soc.*, 1999, **121**, 9245; J. D. Corbett, *Angew. Chem.*, 2000, **112**, 682 (*Angew. Chem., Int. Ed.*, 2000, **39**, 670); S. Scharfe, F. Kraus, S. Stegmaier, A. Schier and T. F. Fässler, *Angew. Chem.*, 2011, **123**, 3712 (*Angew. Chem., Int. Ed.*, 2011, **50**, 3630).
- (a) B. E. Eichler and P. P. Power, *Angew. Chem.*, 2001, **113**, 818 (*Angew. Chem., Int. Ed.*, 2001, **40**, 796); (b) A. F. Richards, B. E. Eichler, M. Brynda, M. M. Olmstead and P. P. Power, *Angew. Chem.*, 2005, **117**, 2602 (*Angew. Chem., Int. Ed.*, 2005, **44**, 2546); (c) L. R. Sita, *Acc. Chem. Res.*, 1994, **27**, 191; (d) C. P. Sindlinger and L. Wesemann, *Chem. Sci.*, 2014, **5**, 2739; (e) E. Rivard, J. Steiner, J. C. Fetting, J. R. Giuliani, M. P. Augustine and P. P. Power, *Chem. Commun.*, 2007, 4919.
- D. J. Chapman and S. C. Sevov, *Inorg. Chem.*, 2008, **47**, 6009; M. W. Hull and S. C. Sevov, *J. Am. Chem. Soc.*, 2009, **131**, 9026; F. S. Kocak,



- P. Y. Zavalij, Y. F. Lam and B. W. Eichhorn, *Chem. Commun.*, 2009, 4197; F. S. Kocak, P. Zavalij and B. Eichhorn, *Chem. – Eur. J.*, 2011, **17**, 4858.
- 12 C. Schrenk and A. Schnepf, *Chem. Commun.*, 2010, **46**, 6756–6758.
- 13 C. Schrenk, A. Kubas, K. Fink and A. Schnepf, *Angew. Chem.*, 2011, **123**, 7411 (*Angew. Chem., Int. Ed.*, 2011, **50**, 7273).
- 14 (a) C. Schrenk, M. Neumaier and A. Schnepf, *Inorg. Chem.*, 2012, **51**, 3989; (b) C. Schrenk, J. Helmlinger and A. Schnepf, *Z. Anorg. Allg. Chem.*, 2012, **638**, 589; (c) C. Schrenk and A. Schnepf, *Main Group Met. Chem.*, 2013, **36**, 161.
- 15 C. Schrenk, F. Winter, R. Pöttgen and A. Schnepf, *Inorg. Chem.*, 2012, **51**, 8583.
- 16 C. Schrenk, B. Gerke, R. Pöttgen, A. Clayborne and A. Schnepf, *Chem. – Eur. J.*, 2015, **21**, 8222; A. Schnepf, *Phosphorus, Sulfur Silicon Relat. Elem.*, 2016, **191**, 662.
- 17 M. Brynda, R. Herber, P. B. Hitchcock, M. F. Lappert, I. Nowik, P. P. Power, A. V. Protchenko, A. Ruzicka and J. Steiner, *Angew. Chem.*, 2006, **118**, 4439 (*Angew. Chem., Int. Ed.*, 2006, **45**, 4333).
- 18 N. J. Hardman, B. E. Eichler and P. P. Power, *Chem. Commun.*, 2000, 1991; N. J. Hardman and P. P. Power, *ACS Symp. Ser.*, 2002, **822**, 2; C.-H. Chen, M.-L. Tsai and M.-D. Su, *Organometallics*, 2006, **25**, 2766; M. S. Hill, P. B. Hitchcock and R. Pontavornpinyo, *Dalton Trans.*, 2005, 273; N. J. Hardman, P. P. Power, J. D. Gorden, C. L. B. Macdonald and A. H. Cowley, *J. Chem. Soc., Chem. Commun.*, 2001, 1866; C. Gemel, T. Steinke, M. Cokoja, A. Kempter and R. A. Fischer, *Eur. J. Inorg. Chem.*, 2004, 4161.
- 19 G. Prabusankar, A. Kempter, C. Gemel, M.-K. Schröter and R. A. Fischer, *Angew. Chem.*, 2008, **120**, 7344 (*Angew. Chem., Int. Ed.*, 2008, **47**, 7234).
- 20 Structural details are given in the ESI†.
- 21 S. Yao, K. W. Klinkhammer and Y. Xiong, *Angew. Chem.*, 2004, **116**, 6328 (*Angew. Chem., Int. Ed.*, 2004, **43**, 6202).
- 22 P. Pyykkö and M. Atsumi, *Chem. – Eur. J.*, 2009, **15**, 186.
- 23 M. Mantina, A. C. Chamberlin, R. Valero, C. J. Cramer and D. G. Truhlar, *J. Phys. Chem. A*, 2009, **113**, 5806.
- 24 J. A. Lee and G. V. Raynor, *Proc. Phys. Soc., London, Sect. B*, 1954, **67**, 737, ICSD entry 40038.

